Story loss functions for seismic design and assessment: Development of tools and application

Davit Shahnazaryan, M.EERI(iD)**, Gerard J O'Reilly**(iD)**, and Ricardo Monteiro**

Abstract

Performance-based earthquake engineering (PBEE) has become an important framework for quantifying seismic losses. However, due to its computationally expensive implementation through a typically detailed component-based approach (i.e. Federal Emergency Management Agency (FEMA) P-58), it has primarily been used within academic research and specific studies. A simplified alternative more desirable for practitioners is based on story loss functions (SLFs), which estimate a building's expected monetary loss per story due to seismic demand. These simplified SLFs reduce the data required compared to a detailed study, which is especially true at a design stage, where detailed component information is likely yet to be defined. This article proposes a Python-based toolbox for the development of user-specific and customizable SLFs for use within seismic design and assessment of buildings. It outlines the implementation procedure alongside a comparative demonstration of its application where dependency and correlation of damage states between different components are considered. Finally, a comparison of SLF-based and component-based loss estimation approaches is carried out through the application to a real case study school building. The agreement and consistency of the attained loss metrics demonstrate the quality and ease of the SLF-based approach in achieving accurate results for a more expedite assessment of building performance.

Keywords

PBEE, seismic assessment, loss estimation, story loss function, correlations

Date received: 3 November 2020; accepted: 18 May 2021

Scuola Universitaria Superiore, IUSS Pavia, Pavia, Italy

Corresponding author:
Davit Shahnazaryan, Scuola Universitaria Superiore, IUSS Pavia, 27100 Pavia, Italy.
Email: davit.shahnazaryan@iusspavia.it

Introduction

Performance-based earthquake engineering (PBEE) (Cornell and Krawinkler, 2003) is widely recognized as a fundamental framework for characterizing seismic risk, using terms that are more meaningful to stakeholders and practitioners. These performance measures can be subdivided into three categories: losses, downtime, and casualties/fatalities. Instead of describing performance at discrete hazard levels, as is typically prescribed in design codes (e.g. American Society of Civil Engineers (ASCE) 7-16, 2016; Comité Européen de Normalisation (CEN) EN 1998-1, 2004; NZS 1170.5:2004, 2004), it acts as a fully probabilistic framework with the inclusion of uncertainties for hazard, structural response, damage, and monetary loss.

Due to the probabilistic nature of the framework and its computationally expensive implementation, it has become popular primarily within academic research or specialized reports, such as FEMA P-58-1 (2012a), rather than a widespread code-based implementation for practitioners. This is especially true for the design of new structures, as practitioners may be hesitant to carry out a full loss-driven design consisting of many trials and iterations. For the seismic assessment of existing buildings, a full inventory of all the building components may be known, but for new designs, this information is yet to be identified. Moreover, many researchers have developed risk-targeted design methods over the years (Aschheim and Black, 2000; Cornell, 1996; Kennedy and Short, 1994; Krawinkler et al., 2006; Luco et al., 2007; O'Reilly and Calvi, 2019; Shahnazaryan and O'Reilly, 2021; Vamvatsikos and Aschheim, 2016; Žižmond and Dolšek, 2019). Risk-targeted approaches use collapse risk as the primary design objective, while others (Krawinkler et al., 2006; O'Reilly and Calvi, 2019; Shahnazaryan and O'Reilly, 2021) explore the possibility of utilizing economic loss. To simplify the codification of these approaches, where lack of initial data are inevitable, alternatives are sought.

A simplified alternative to PEER's building-specific loss estimation methodology was developed by Ramirez and Miranda (2009). The idea was to create engineering demand parameter versus decision variable (EDP–DV) functions, which relate the structural response parameters, or EDPs, directly to economic losses, or DVs. These functions typically define monetary loss at a story level hence are termed story loss functions (SLFs). They reduce the computational effort by providing ready-made loss functions that describe the repair costs over a predefined building inventory of damageable components in a simplified manner. They, therefore, reduce the amount of data required to be handled for the building's inventory when estimating losses. As stated previously, this is particularly important at the design phase, where the components of the building are not known in great detail. Generic SLFs would help minimize this issue by reducing the excessive computational effort required in component-based approaches. These SLFs have been recently implemented, for instance, in Silva et al. (2020b) for steel buildings in a European context, whereas suitable options for reinforced concrete (RC) buildings are still missing. Furthermore, the possibility for users to tailor and personalize their damageable inventories, repair actions, and repair costs to arrive at more fine-tuned SLFs is also currently unavailable.

The approach utilized in this study is based on the story loss estimation framework by Ramirez and Miranda (2009), which is used to develop a toolbox for creating generic user-based SLFs. Component quantities, fragility, and consequence functions are used as input components to generate FEMA P-58-1 (2012a) compatible SLFs. The method proposed by Ramirez and Miranda (2009) uses the 2007 RS Means Square Foot Costs (Balboni,

2007), applicable to the United States only, to estimate the building cost distributions for different RC building occupancies in California. The main difference of the more recent proposal by Papadopoulos et al. (2019) was the use of the FEMA P-58-1 (2012a) database, where the functions were customizable with respect to replacement cost and to reflect building's floor area. The functions developed by Papadopoulos et al. (2019) were developed for steel buildings in Greece; however, no damage or spatial correlation was considered among the different components, as opposed to the former approach. To aid the generation of EDP–DV functions or loss assessment in general, significant research has been carried out with the goal of developing fragility and consequence functions for various structural and non-structural components. For example, fragility and consequence functions were developed for unreinforced masonry (URM) buildings by Ottonelli et al. (2020), many others have focused on masonry infill walls (Cardone and Perrone, 2015; Chiozzi and Miranda, 2017; Del Gaudio et al., 2019; Ruiz-García and Negrete, 2009; Sassun et al., 2016), while some concentrated on developing functions for RC structural components (Aslani and Miranda, 2005; Cardone, 2016). Furthermore, recent studies on loss estimation (Perrone et al., 2019; Sullivan, 2016) highlighted the need for developing SLFs to cover a wide range of building characteristics (i.e. story-wise functionality, typology of structure, occupancy, and use of a building). Sullivan (2016) presented a simplified loss assessment approach to calculate the expected annual loss (EAL), which could act as a quick estimation tool for identifying necessary design or retrofit choices early in a project and effectively reduce the monetary costs. However, a limitation was highlighted, whereby the knowledge of quantity, distribution, and characteristics of all damageable components within the building inventory might not always necessarily be readily available and, to address it, SLFs could be used. On the contrary, Perrone et al. (2019) proposed a method for estimating EAL of Italian RC buildings, which also utilizes suitable SLFs, further demonstrating the need to develop simplified alternatives.

The aim of this study is to present a toolbox that allows the automated production of SLFs through regression analysis using the results of random sampling of component damage states (DSs) and costs, including damage correlation among components. The goal is not the development of generic loss functions for specific building occupancies but the development of a tool for practitioners to create their own functions, based on their needs using an existing database of components, such as FEMA P-58 or any other means (e.g. expert judgment), without being limited to existing SLF libraries. The framework implemented within the toolbox is outlined in this study and an example application is presented. The main decisions to be made before using the toolbox include the building characterization through the definition of the component inventory, defined by component quantities, fragility, and consequence functions; performance grouping of components based on EDP sensitivity; identification of possible interactions among various components; choice of the number of simulations for the sampling of DSs; and choice of regression fitting type. Finally, the framework is validated via a case study application to an existing school building, and the results are compared with a component-based loss assessment of the same building.

Development of an SLF estimation toolbox

The framework utilized herein defines SLFs as based on component inventories and their classification into different component groups. For the proper estimation of repair costs
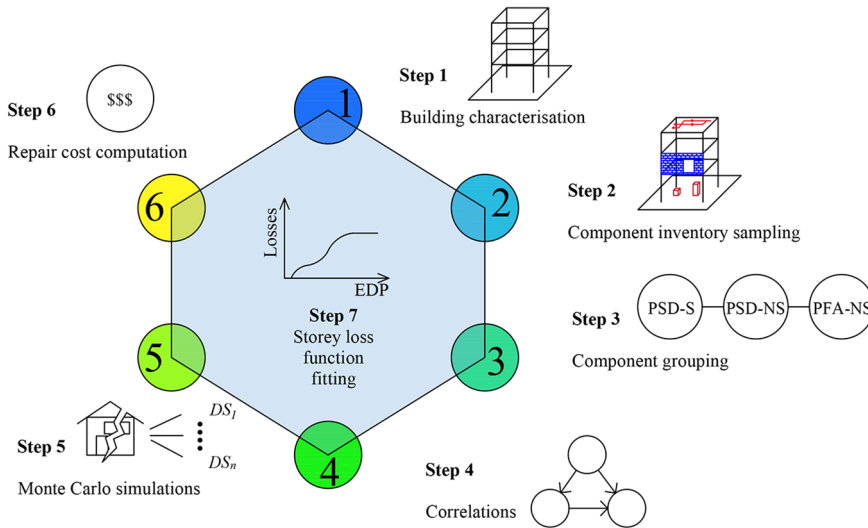
Figure 1. Flowchart of story loss function generation framework.

associated with each component, consistent integration of component fragilities with repair costs at the story level is carried out. The framework consists of the following steps (Figure 1):

1. Building characterization;
2. Component inventory definition;
3. Component grouping;
4. Consideration of correlations between components;
5. Monte Carlo simulation of DSs;
6. Repair cost computation;
7. Story loss function fitting.

Step 1: building characterization

The first step of the framework foresees examining the characteristics of the building of interest. The user should have relevant information on the structure's height, namely number of stories, global dimensions, occupancy type, and usage. In many situations, the building's components will vary on a story-by-story basis (i.e. the components will not necessarily be identical in type and quantity at the ground floor, roof level, and intermediate stories). For example, the contents of the ground story of a residential building may vary significantly in terms of structural and non-structural components compared to upper stories, since this may comprise commercial space or car parking. In contrast, the roof level generally includes components, such as HVAC (heating, ventilation, and air conditioning) equipment or necessary equipment for geared elevators, which are not located at other stories. All such considerations need to be made to arrive at a comprehensive description of the building's characteristics and where the damageable components are distributed.

Step 2: component inventory

Once the occupancy type, structural typology, and other specific building characteristics have been established, the damageable component inventory can be created. There are several methods to aid the user to gain insight into the possible distribution of components if it is not preliminarily known, as is the case for new designs. The distributions, which assume knowledge of mean and uncertainty of a given component quantity, may be obtained from empirical and statistical data, collected from existing buildings and surveys, or based on expert opinion or personal judgment when such information is unavailable. The inventory consists of structural, non-structural components, and story contents likely to be damaged, which contribute to the economic losses associated with required repair costs.

In general, the component data inventory should have information on item types, quantity of each component, EDP sensitivity, and typology (structural or non-structural) of each component. Three performance groups are to be identified unless otherwise specified, and fragility and consequence functions for the components should be available. To define the component database, DSs with corresponding fragility and consequence functions accounting for best fitting function suggestions (e.g. normal, lognormal, etc.) may be adapted from the FEMA P-58 database or other similar sources.

Another consideration to account for is to distinguish whether certain components will be affected by the peak floor acceleration (PFA) of the floor slab above the current story or by the supporting floor slab. For instance, the water distribution piping system connected to the ceiling in a story will be sensitive to the PFA of the above floor, while contents (e.g. electronic equipment or contents) will be sensitive to the PFA of the supporting floor. To account for this, a simplifying assumption is made in the tool. The component losses in the story i, but affected by the upper floor, are computed as part of, or moved to, story $i + 1$. This essentially means that the estimation of total costs in the building is theoretically correct, but the physical location of the costs is not (i.e. a story i component loss sensitive to PFA of the floor above will see its cost be logged as story $i + 1$ losses). This assumption was deemed suitable when considering the alternative simplifying assumption of utilizing the incorrect PFA demand at story i, and subsequently an incorrect loss, to maintain the correct story location.

Finally, to generate a component inventory in a meaningful manner, it is important to be aware that, during assessment, even if component information is known, it might not be possible to count the entire physical inventory precisely. A distinction could be made concerning the reference area used for the component inventory. For that purpose, as in FEMA P-58, an approach assuming quantities per meter squared may be applied, which are then scaled to a unit area (e.g. 100 m^2). Then, by counting only the stock of individual components, the quantities are extrapolated to arrive at an estimated amount of a component type within a story. However, this is only applicable to components whose inventory is large enough and when the counted components are representative. For example, elevator or HVAC systems are specific to certain locations of the building (i.e. neither distributed along with the height nor the area of the building). Hence, in this case, scaling per meter square will not be applicable and unitary estimates based on floor area thresholds should be considered instead.

The framework adopted in this study assumes two-dimensional (2D) structural modeling, where the damageable components are oriented in the same direction. However, should one apply the framework to three-dimensional) 3D buildings, the SLFs could be

calculated by making assumptions on how the building components of different orientations are distributed. In particular, functions for both directions of a story for that specific component could be developed. Essentially, the framework could be applied in each direction separately with appropriate care and consideration. To be specific, the analyst would need to identify, for each damageable component considered at each story level, in which principal direction of the building it is sensitive to damage. This way, the components can be grouped and analyzed separately using the structural demands in the two orthogonal directions. Furthermore, in the case of non-directional components, such as the acceleration-sensitive non-structural components analyzed in the case study building, where both directions of the seismic action are of importance, the maximum value of the two demand parameters in both directions may be multiplied by a non-directional conversion factor, as suggested in FEMA P-58, and used for a single SLF in the analysis. However, similar to components located on different stories and within different performance groups, interactions of seismic effects in the two directions on a given component are not accounted for and in cases where such interaction is expected to be significant, more advanced methods of loss assessment should be adopted.

Step 3: component grouping

Once the component inventory has been identified, depending on the type of components (i.e. structural or non-structural) and their sensitivity to a specific EDP (i.e. to peak story drift (PSD) or PFA), the components are classified into performance groups. Three performance groups are established: PSD-sensitive structural, PSD-sensitive non-structural, and PFA-sensitive non-structural components. Components within a performance group will be assessed together for a mutual demand and subsequent losses will be summed up to estimate the group's SLF. In other words, losses from all components within a performance group will be tied to the same EDP.

As in the case of similar past studies (Papadopoulos et al., 2019; Ramirez and Miranda, 2009), the effects of other EDPs, such as vertical acceleration or building torsion, are not accounted for herein. In addition, torsion could be better dealt with adopting a component-based approach, as discussed in O'Reilly et al. (2017). However, it is important to keep in mind that if one is to provide the toolbox with fragility and consequence functions associated with components other than PSD or PFA sensitive (e.g. peak floor velocity, PFV), the toolbox will still be capable of producing the corresponding desired SLFs.

In addition to having a separation between different component typologies, the classification into performance groups allows the disaggregation of losses at the later stages to identify the main contributors to the economic losses. This is especially important for visualization purposes, as the loss contribution from collapsing and non-collapsing cases may be easily established along with loss contributions of individual stories and performance groups (e.g. structural and non-structural components).

Step 4: consideration of correlations between components

Structural and non-structural components that are sensitive to the same EDP may be grouped to allow the consideration of possible correlations between different performance groups. For example, even though a specific intensity level might not entail damage to a specific non-structural component alone, a structural component connected to it might be
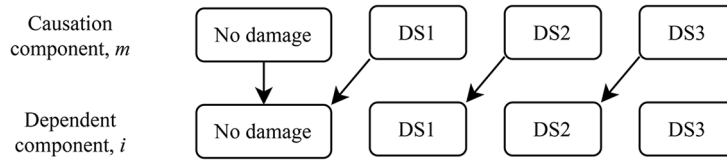
Figure 2. Relationship between causation and dependent components.

damaged. This means that to repair the structural component, access should be first granted, which foresees the removal of the portion or the entirety of the undamaged non-structural component. When dependencies are considered, it was shown (Ramirez and Miranda, 2009) that there may be an error if the repair cost of the dependent component is counted twice. For example, the columns in a moment-frame building and internal partitions may be damaged but the repair cost of a dependent component may be counted twice (the so-called double-counting). Hence, care should be taken to provide proper repair costs and to establish correct relationships between components that best align with their actual physical relationship. Essentially, for any component i, if it is not dependent on any other component, then all its DSs are assumed to have an independent sequential occurrence unless otherwise specified and each DS is assumed to be mutually exclusive (i.e. the occurrence of one damage state means that the other ones will not happen). A probability of occurrence is assigned (see Step 5) to mutually exclusive DSs, which sums up to 100%. Otherwise, if DS j of component i is also dependent on the occurrence of a DS d of a component m, then the DS of component i is assumed independent of component m unless component m is in DS d or higher (i.e. DS d in component m triggers DS j in component i). For dependent components, this triggered DS, DS_{trig}, is identified, which is based on the causation DS of another component, as illustrated in Figure 2. In the example, for an EDP of edp, once the causation component m is in DS3, even if the fragility parameters of the dependent component i do not indicate any damage, it will still be in DS2, as it depends on the DS of component m (i.e. the dependent component's triggered DS is DS2). Analogously, if component m is in DS2, then the triggered DS of i is DS1.

Step 5: Monte Carlo simulation of DSs and repair costs

With the component inventory identified, along with the fragility and consequence functions and possible correlations among the DSs of different components, Monte Carlo simulations are performed. For each simulation, damage and repair costs are sampled for each component of the performance group and each cost is added to obtain the performance group's total loss for a given EDP. Figure 3 presents a flowchart illustrating the algorithm for the estimation of SLFs. For both uncorrelated components, where independence of each component is assumed, and in case of existing correlation among different component types, the algorithm samples DSs for each component at each EDP level and a specified number of simulations. Essentially, a random value is generated between 0 and 1 representing the probability of being in a DS; then, a DS is assigned to a component based on its fragility functions (Figure 4). This process, described in Step 4, is repeated for each dependent component for the population of the DS matrix. For example, to assign a DS to a component from the simulations, if EDP = 0.02 (point 1 in Figure 4) and the
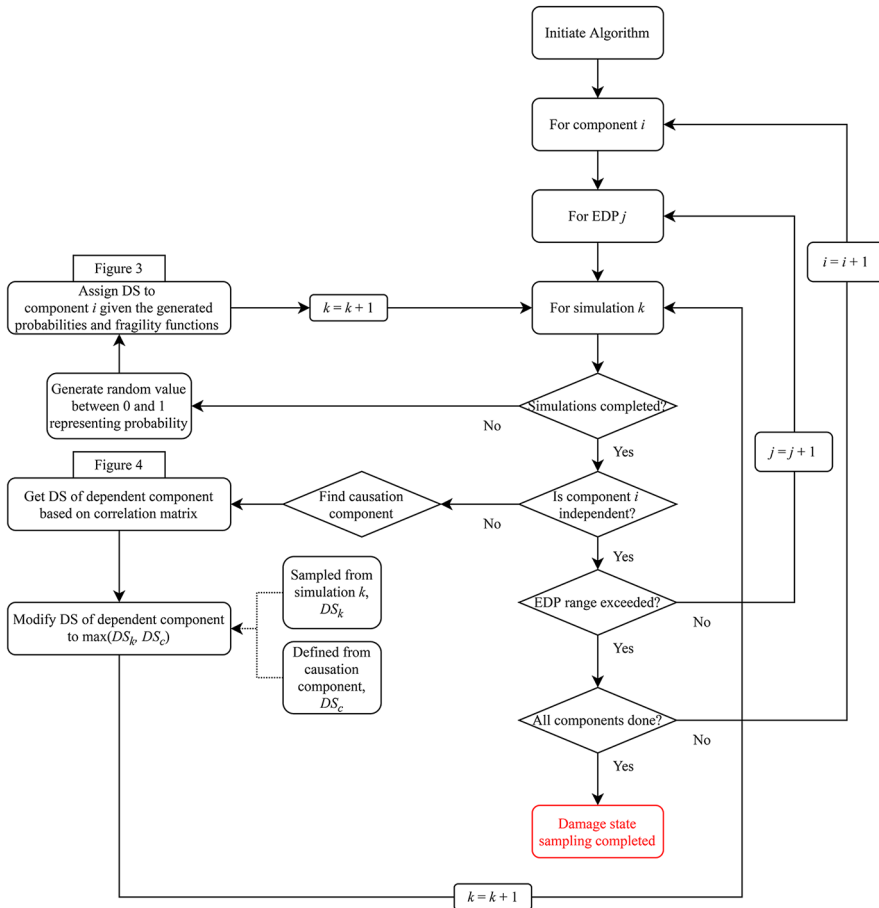
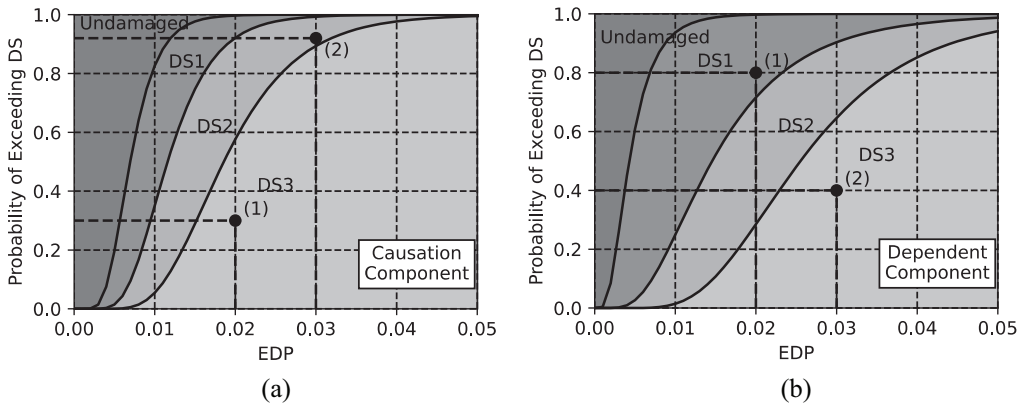**Figure 3.** A sampling of damage states using Monte Carlo simulation.

Figure 4. Damage states and fragility functions of a sample (a) causation component and (b) dependent component.
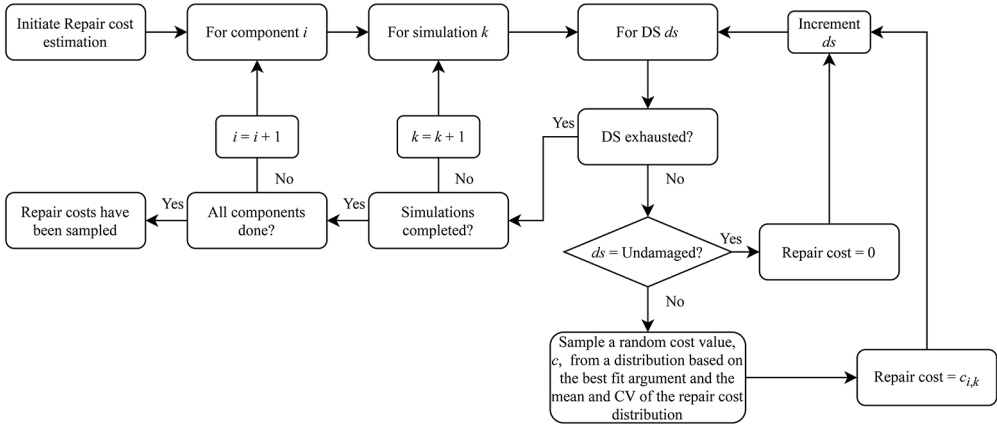
Figure 5. Assignment of component repair costs based on sampled damage states.

sampled probability for the causation component is 0.3, then DS3 is assigned to the component. In the same example, the sampled probability for the dependent component is 0.8 for EDP = 0.02, meaning that DS1 is assigned. Following the relationship of the components described in Figure 2, the DS of the dependent component is modified to DS2. Alternatively, for EDP = 0.03 (point 2 in Figure 4), if through the same process DS2 and DS3 are assigned to the causation and dependent components, respectively, following the relationship in Figure 2, no modifications would be required.

Step 6: repair cost computation

With the DSs assigned to the components per Monte Carlo simulation, repair costs may be evaluated (Figure 5). For each component at each sampled DS, repair costs are assigned based on the provided consequence functions. In case the consequence function is represented solely through the mean value, then the mean value is assigned. If a distribution of the repair cost is provided (i.e. mean and standard deviation if normally distributed or median and dispersion for lognormal distributions), then a random value is sampled from the distribution and a corresponding repair cost is assigned to consider the uncertainty in estimating repair costs also.

To normalize the repair costs, a replacement cost of the building, *ReplCost*, should be provided by the user or else be set equal as unity, meaning that no normalization is carried out. The previously identified repair cost of component i at simulation k, $c_{i, k}(q_i)$, may then be normalized using Equation 1:

$$\hat{C}_{i, k} = \frac{c_{i, k}(q_i)}{ReplCost} \tag{1}$$

where $\hat{C}_{i,k}$ is the normalized repair cost of component i at simulation k and q_i is the quantity of component i, of which the repair cost is a function (i.e. the repair cost per unit may decrease with increased units). As illustrated in Figure 6, based on q_i, the mean repair cost, c_i, is obtained, which is used in conjunction with the coefficient of variation, *cov*, for
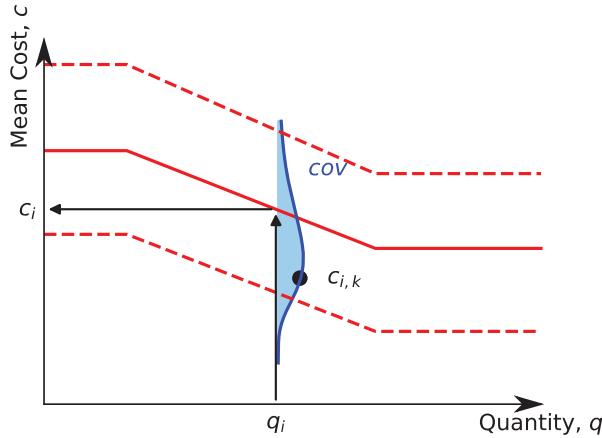
Figure 6. Consequence function describing the relationship of repair cost as a function of quantity.

generating a normal distribution of repair cost. Finally, a value of $c_{i,k}(q_i)$, is randomly sampled from the distribution.

Then, the total normalized repair cost at simulation k, for component i, $\hat{C}_{total,i,k}$, is computed through a summation of the repair costs of all the components according to Equation 2:

$$\hat{C}_{total,i,k} = \hat{C}_{i,k}q_i \tag{2}$$

The normalized total repair cost of story st at simulation k, $\hat{C}_{st,k}$, will be the sum of normalized repair costs of all components at that story, as per Equation 3:

$$\hat{C}_{st,k} = \sum_{i=1}^{m} \hat{C}_{total,i,k} \tag{3}$$

where m is the number of component types within the story inventory.

Step 7: storey loss function fitting

With the component inventory defined and classified into performance groups, along with the consideration of possible correlations among various components, the SLFs for component groups may be identified through regression analysis on the normalized repair costs sampled. More than one analytical expression may be used within the toolbox, while possible addition of new functions may be considered, as future research identifies better alternatives. The Weibull cumulative distribution function may be used to perform the regression, which is defined in Equation 4:

$$y = \alpha \left(1 - \exp\left(-\left(\frac{x}{\beta} \right)^{\gamma} \right) \right) \tag{4}$$

where, α, β, and γ are the fitting coefficients, x is the EDP value, and y is the fitted loss ratio value.

Alternatively, the regression model proposed by Papadopoulos et al. (2019), defined in Equation 5, may be used:

$$y = \varepsilon \frac{x^\alpha}{\beta^\alpha + x^\alpha} + (1 - \varepsilon) \frac{x^\gamma}{\beta^\gamma + x^\gamma} \tag{5}$$

where, α, β, γ, δ, and ε are the fitting coefficients of the regression analysis, x is the EDP, and y is the fitted loss ratio. The accuracy of the regression is then gauged through the estimation of maximum, $error_{max}$, and cumulative, $error_{cum}$, relative regression errors over the EDP range for each component performance group, according to Equations 6 and 7:

$$error_{max} = \max\left(\frac{\left| C_{repair}^{EDP} - \hat{C}_{repair}^{EDP} \right|}{\max\left(C_{repair}^{EDP} \right)} \right) \tag{6}$$

$$error_{cum} = \int_{0}^{EDP = \max EDP} \left(\frac{\left| C_{repair}^{EDP} - \hat{C}_{repair}^{EDP} \right|}{\max\left(C_{repair}^{EDP} \right)} \right) dEDP \tag{7}$$

where C_{repair}^{EDP} and $\hat{C}_{repair}^{EDP}$ are the original and fitted repair costs, respectively.

Summary

The proposed framework yields, as main outputs, SLFs for each performance group (Figure 1). Loss estimation can then be carried out similar to the FEMA P-58 guidelines, which utilizes a probabilistic approach for estimation of damage and corresponding loss. The losses are scaled based on the unit area considered, which could be a small portion of the story area or the total area of the story.

While the total loss may be expressed via a monetary measure such as dollars or euros, one may opt to normalize the fitted SLFs with respect to the total story cost (Equation 1), so that they may be scaled or converted to match the common standards of any country. However, attention should be paid to how and where from the component fragility and consequence functions are obtained, given that the data from FEMA P-58, when used outside the United States, even if scaled by a conversion factor, might not be appropriate. In such cases, a rational conversion specific to a country, as proposed by Silva et al. (2020a), is recommended.

The final stage of estimating SLFs involves a regression on the generated data to obtain the fitted curves, which may be carried out assuming Equations 4 or 5. The tool itself is implemented in a Python script (Shahnazaryan et al., 2021). Figure 7 illustrates the program structure of the entire SLF generator module and Figure 8 presents an overview of the main interface of the toolbox.

Characterization of case study building

For the demonstration of the toolbox and generation of EDP–DV functions, a case study building was adopted from O'Reilly et al. (2018) for a testing and validation exercise to be compared with component-based assessment following the FEMA P-58 guidelines. For this, typical cost distributions for the case study building need identification. The selected

Input

External files   Internal choices

| **Component information:** Building component and cost distributions Component correlations as *.csv files | Correlation type | Regression function type | EDP bin widths | Number of Monte Carlo simulations |
| | Repair cost conversion factor | Replacement cost | Performance grouping | |

SLF generation toolbox

Methods:
get_edp_range()   *derive_fragility_functions()*   *perform_regression()*
get_component_data()   *perform_Monte_Carlo()*   *compute_accuracy()*
group_components()   *assign_ds_to_dependent()*
get_correlation tree()   *calculate_costs()*

Outputs

Main: **Cache:**
SLF functions   *SLF functions*
Fitting parameters   *Damage States*
Accuracy metrics   *Complete cost calculations*

Figure 7. Programming structure of the SLF generation toolbox.
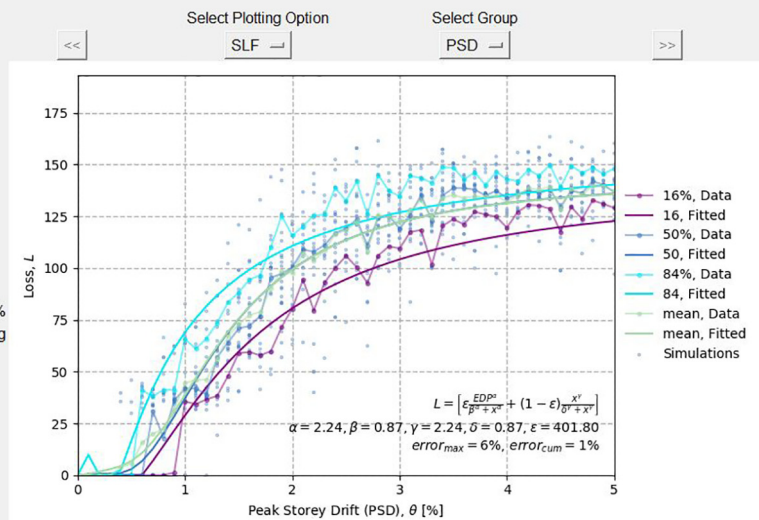
Figure 8. Overview of the story loss function generator interface.

Figure 9. Main geometrical and structural properties of the case study building adapted from O'Reilly et al. (2019).

school building, constructed in the 1960s, consists of three stories and has an RC frame with masonry infills as the lateral force-resisting system. The aforementioned study (O'Reilly et al., 2018) provides the distribut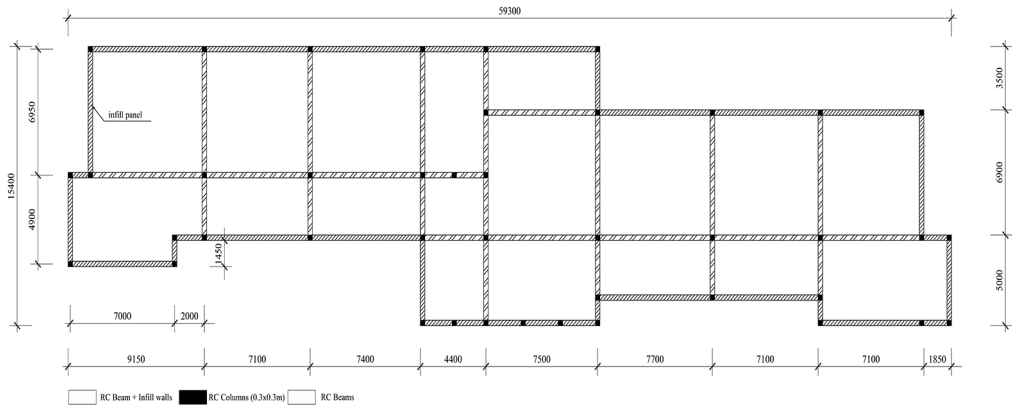ion of the structural and non-structural components, their fragility, and consequence functions. Figure 9 illustrates the structural configuration of the case study building. The building has RC square columns of 30 cm and beams of 30 × 50 cm, which were designed for gravity loads only. Infills were identified as double leaf 12 cm hollow clay brick with a 5 cm wide internal cavity and the floor systems were identified as "laterizio" found commonly in Italy at that time of construction. The following sub-sections address the primary details and assumptions associated with the component data inventory selected and how inputs are created for the toolbox to generate SLFs.

Building components and cost distributions

The second story (intermediate story) of the case study building was selected here for the demonstrative analysis comparing SLF generation, assuming both independence and correlation of some components. However, the toolbox was also applied to generate SLFs for the whole structure and loss assessment was carried out to validate the results with respect to a component-based approach. Cost distributions for the structural and non-structural components and detailed component inventory with quantities were adopted from O'Reilly et al. (2018). Tables 1 and 2 summarize the mean structural and non-structural component quantities, respectively. The tables identify the type of the component, the demand parameter that the component is sensitive to, the unit for measuring the quantity of the component and the quantities of each type of component. For structural components, PSD is assumed as the EDP, while for non-structural components, the main EDPs are both PSD and PFA.

For the sake of brevity, only PFA- and PSD-sensitive components were analyzed. Only the bookcases were defined as sensitive to the PFV demand parameter (O'Reilly et al., 2018) so it was decided to omit it from this study and reimplement the component-based approach without it. Moreover, PFA-sensitive components were grouped depending on the location within a story and to which EDP they were sensitive. That is, components such

Table 1. Mean quantities for the damageable structural components of the case study school building in the longitudinal direction (quantities for the transverse direction listed in parenthesis)

ID	Component	Demand parameter	Unit	Quantity per story		
				Story 1	Story 2	Story 3
A101	Exterior beam–column joints (end-hooks)	PSD (%)	per unit	20 (26)	20 (26)	20 (26)
A104	Interior beam–column joints (weak columns)			23 (15)	23 (15)	22 (14)
A110	Ductile weak columns (lapped)			44	44	44
A121	Exterior masonry infill (with windows)		per m^2	454.5 (127.77)	454.5 (127.77)	447.4 (125.8)

PSD: peak story drift.

as piping systems located in a story i but sensitive to the EDP of the above story were tied to the PFA of story $i+1$, while components such as computers located in the story i that are not sensitive to the above EDP were tied to the PFA of story i, as described previously.

Component fragility and consequence functions

Creating EDP–DV functions requires the definition of fragility and consequence functions for all components considered. Tables 3 and 4 provide the damage descriptions, the sources for the function definitions, and the fragility function parameters for non-structural and structural components, respectively. For the RC structural components, fragility functions were adopted from the available literature (Cardone, 2016; Cardone and Perrone, 2015). For the non-structural components, the fragility functions were adopted from Sassun et al. (2016) for the masonry infills, while the remaining component fragility functions were adopted from FEMA P-58-1 (2012a) and the components were assumed as PFA-sensitive.

For some non-structural components, specific fragility functions were not available, hence O'Reilly et al. (2018) assumed that the damage to, for example, doors, windows, desks, or chairs, was directly correlated to the collapse DS of the internal infill walls (i.e. DS4). The assumption was that the dependent components are generally either placed within or adjacent to the causation component (i.e. the internal infill walls in this particular scenario). This sort of indirect fix is also an example of the kind of situations that can be dealt with appropriate correlation models. The last column of Tables 3 and 4 defines the mean repair costs as a function of the quantity of components and associated with the DS of each component within the structural and non-structural component inventory, respectively. As per O'Reilly et al. (2018), repair costs were defined assuming a normal distribution with coefficient of variation equation to 0.1. A full spatial correlation was assumed among the components of the same type within the same story.

In other words, if a given DS of an exterior beam–column joint is recorded, the assumption is that the repair cost is the summation of the repair costs of all exterior beam–column joints. However, in practice, it is unlikely that every single component of the same type will be damaged identically within the story for the given level of EDP. For a more realistic evaluation, a scaling factor smaller than 1.0 can be applied to reduce the costs through

Table 2. Mean quantities for the damageable non-structural components of the case study school building in the longitudinal direction (quantities for the transverse direction listed in parenthesis)

ID	Component	Demand parameter	Above EDP	Unit	Quantity per story		
					Story 1	Story 2	Story 3
A123	Internal masonry partition	PSD (%)	No	per m²	198.9 (65.9)	198.9 (65.9)	195.7 (64.8)
A200	Stairs (C2011.011b)		No	per unit	—	—	—
C100	Internal partition		No	per m²	317.8 (335.3)	291.9 (243.6)	268.1 (231.0)
C200	Gypsum infill walls with metal studs		No	per m²	198.9 (65.9)	198.9 (65.9)	195.7 (64.8)
C300	Doors		No	per unit	18 (15)	13 (10)	15 (10)
C400	Windows		No		23 (17)	50 (9)	53 (9)
C500	Desks		No		110	145	182
C600	Chairs		No		140	182	182
E100	Home entertainment equipment (E2022.020)	PFA (g)	Yes		28	30	30
E1000	Suspended ceiling systems (C3032.001b)		Yes	per m²	560	588	566
E110	Switchboards (D3067.011a)		No	per unit	1	3	3
E200	Lights (C3034.001)		Yes		66	48	48
E300	Water distribution piping systems (D2022.011a)		Yes	per 250 m	1.808	1.808	1.808
E400	Heating distribution piping systems (D2022.011a)		Yes		1.904	1.904	1.904
E600	Mobile blackboard (E2022.020)		No	per unit	3	3	4
E700	Electronic blackboard (E2022.020)		No		0	3	3
E800	Personal computer and printer (E2022.023)		No		6	20	0
E900	Independent pendant lighting (C3034.001)		Yes		0	3	3

EDP: engineering demand parameter; PSD: peak story drift; PFA: peak floor acceleration.

Table 3. Fragility function parameters and repair costs for non-structural components of the second story

ID	Damage states (DSs)	Source	Fragility function parameters		Mean repair cost €
			Median (% for PSD, g for PFA)	Dispersion	
A123	DS1 light cracking DS2 extensive cracking DS3 collapse	Cardone and Perrone (2015)	0.15 0.40 1.00	0.50 0.50 0.40	62 117 234
A200	DS1 non-structural damage DS2 structural damage DS3 loss of live load capacity	FEMA P-58-3 (2012b)	0.50 1.70 2.80	0.60 0.60 0.45	683 5868 36399
C100	DS1 operational DS2 damage limitation DS3 significant damage DS4 near collapse limit state	Sassun et al. (2016)	0.18 0.46 1.05 1.88	0.52 0.54 0.40 0.38	35 62 124 124
C200	DS1 operational DS2 damage limitation DS3 significant damage DS4 near collapse limit state		0.18 0.46 1.05 1.88	0.52 0.54 0.40 0.38	62 117 234 234
C300 C400 C500 C600	DS1 damaged DS1 damaged DS1 damaged DS1 damaged	O'Reilly et al. (2018)	1.88 1.88 1.88 1.88	0.38 0.38 0.38 0.38	754 347 191 24
E100	DS1 falls, does not function	FEMA P-58-3 (2012b)	0.80	0.40	1035
E1000	DS1 5% of tiles dislodge and fall DS2 30% of tiles dislodge and fall DS3 total ceiling collapse		0.55 1.00 1.50	0.40 0.40 0.40	49 69 99
E110	DS1 damaged, inoperative		0.69	0.40	5569
E200	DS1 disassembly of rod system at connections with horizontal light fixture, low cycle fatigue failure of the threaded rod, pull-out of rods from ceiling assembly		1.00	0.40	583
E300 E400	DS1 small leakage of joints DS2 large leakage w/ major repair		0.55 1.10	0.40 0.40	307 2302
E600 E700 E800 E900	DS1 falls, does not function		0.80 0.80 0.40 0.60	0.40 0.40 0.40 0.40	297 2162 1913 1627

PSD: peak story drift; PFA: peak floor acceleration; FEMA: Federal Emergency Management Agency.

Table 4. Fragility function parameters and repair costs for structural components of the second story

ID	Damage states (DSs)	Source	Fragility function parameters		Mean repair cost
			Median (% for PSD, g for PFA)	Dispersion	
A101	DS1 light cracking	Cardone (2016)	0.75	0.40	1284
			1.25	0.40	2155
			2.00	0.40	2895
A104	DS2 concrete spalling		0.65	0.40	1497
			1.75	0.35	2574
			3.00	0.30	4041
A110	DS3 concrete crushing		0.75	0.40	882
			1.75	0.35	1388
			3.00	0.35	1747
A121	DS1 light cracking	Cardone and Perrone (2015)	0.10	0.50	62
	DS2 extensive cracking		0.30	0.50	117
	DS3 corner crushing		0.75	0.40	234
	DS4 collapse		1.75	0.35	234

PSD: peak story drift; PFA: peak floor acceleration.

engineering judgment to gauge what fraction of the total will actually be damaged, which may be applied within the toolbox, if desired.

Correlated components

Consideration was given here for possible correlations among DSs of different components in the considered case study school building. Doors, windows, desks, and chairs were already tied to the collapse DS of the infill walls. However, for demonstration purposes, logical correlations based on engineering judgment were assigned here among other components within the same EDP-sensitive group. In other words, no correlation was considered between PFA- and PSD-sensitive components; however, correlation among PSD-sensitive structural and non-structural components was considered. The description of the damage of the causation component, as well as its effect on the correlated component, is provided in Table 5.

It is important to note that, specifically for the case study example, the repair action cost of demolition of partitions and their further restorations is included within the consequence function of the causation component (i.e. there might be a possible double counting involved inherently). However, within the context of this study, no action was taken to avoid double counting as the repair cost source data were not available to sufficiently segregate and avoid it. To avoid compromising the accuracy of results of future analyses, it is advised to add correlations of components with proper care in the computation of repair costs to avoid double counting.

Table 5. Example correlation between components of the case study school building examined

Causation component ID	Damage description of causation component	Dependent component ID	Effect on the dependent component	DS of a dependent component
A101	DS2 concrete spalling	A121	Demolition of exterior infills, as necessary	DS3
A104		A123	Demolition of interior partitions, as necessary	
A104		C100		
A104		C200		
A101		A200	Local cracking, localized spalling, and yielding	DS1
A104	DS3 concrete crushing	C300	Damaged, to be replaced	DS1
		C400		
		C500		
		C600		

DS: damage state.

Table 6. Regression parameters for both equations fitted for the intermediate story SLF of the case study school building

Performance group	Equation 4—Weibull			Equation 5—Papadopoulos et al. (2019)				
	α	β	γ	α	β	γ	δ	ε
PSD S	1.00	1.26	1.14	1.38	2.15	1.38	2.16	989.71
PSD NS	1.00	1.65	1.43	1.66	2.88	1.66	2.89	606.70
PFA NS	2.47	0.79	1.94	2.47	0.79	2.47	0.79	340.54

PSD: peak story drift; S: sensitive; NS: non-structural; PFA: peak floor acceleration.

Derivation of SLFs using the toolbox

The framework was initially applied for a comparative analysis between a scenario where no correlation was assumed among different components' DSs and a scenario where the correlation was assumed. For that purpose, the toolbox was applied at the second story of the building.

Estimating SLFs assuming uncorrelated components

The toolbox was initially applied to the second story of the school building assuming no correlation among the DSs of the components. SLFs were estimated using both regression Equations 4 and 5, the parameters of which are provided in Table 6. The curves are quite similar as illustrated in Figure 10. In particular, Figure 10a shows the loss curves for structural components of the intermediate story. Regardless of the regression equation being used, the losses start accumulating at low values of PSD, which is particularly due to low capacities of interior and exterior infills (Table 4). In turn, losses of PSD-sensitivity nonstructural components are given in Figure 10b and, as is seen, the losses are almost twice
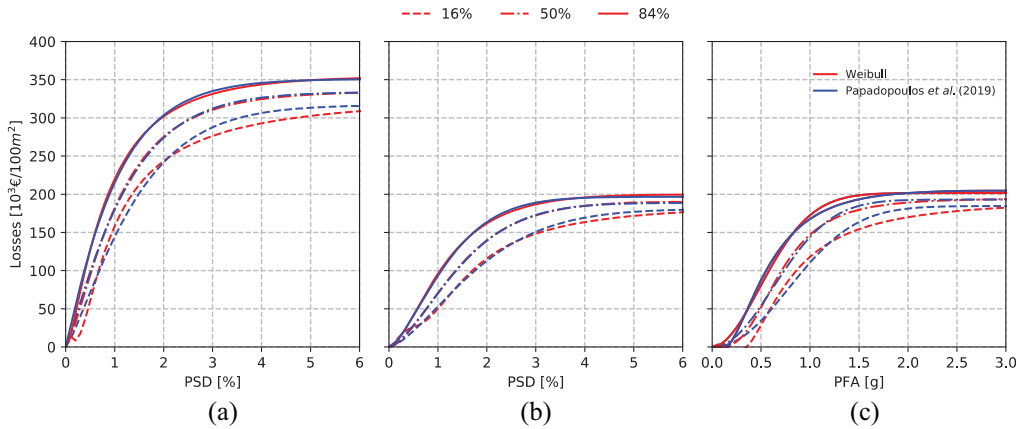
Figure 10. Story loss functions for the case study school building intermediate (second) story level and second floor (Equations 4 and 5). (a) PSD-sensitive structural components, (b) PSD-sensitive non-structural components and (c) PFA-sensitive non-structural components.

Table 7. Accuracy metrics of regression analysis

Performance group	Equation 4—Weibull		Equation 5—Papadopoulos et al. (2019)	
	$error_{max}$ (%)	$error_{cum}$ (%)	$error_{max}$ (%)	$error_{cum}$ (%)
PSD S	5.0	0.1	3.0	0.1
PSD NS	4.5	0.1	5.0	0.1
PFA NS	2.9	4.9	0.7	1.5

PSD: peak story drift; S: sensitive; NS: non-structural; PFA: peak floor acceleration.

as low than the ones associated with the structural components for this particular scenario. Finally, Figure 10c provides the losses associated with non-structural contents.

The regression functions were used to fit the fractiles of the distributions and the accuracy of the regression was then gauged through the estimation of maximum, $error_{max}$, and cumulative, $error_{cum}$, relative regression errors, summarized in Table 7. The results for Equation 4 indicate that, even though a smaller maximum relative error was attained for PFA-sensitive non-structural components, the cumulative relative error is much higher, when compared to the errors of other performance groups, which indicates that, in general, the regression performed worse for the whole data. Nevertheless, Equation 5 required higher computational time, due to more coefficients involved in the fitting process.

Estimating SLFs assuming correlated components

The toolbox was also applied assuming component correlations. Figure 11a depicts the SLFs of PSD-sensitive components at the intermediate story of the case study school building following Equation 4.

For this particular application, the consideration of correlated components did not impact the loss in a significant manner when compared with the independency
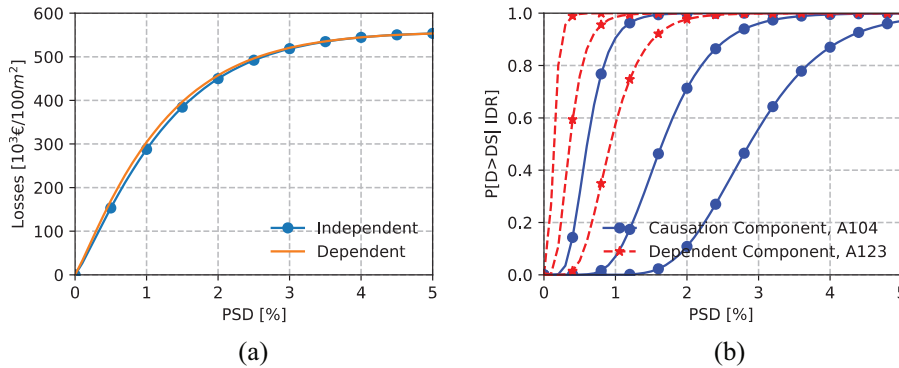
Figure 11. (a) SLFs for the case study school building intermediate story level: PSD-sensitive structural and non-structural components; (b) fragility functions of interdependent components.

assumption, although some increase in vulnerability was noted. This may be attributed to the fragility functions of the components (Figure 11b), where no notable overlap is observed between the fragility function of the causation and dependent component. In addition, the dependent component seems to have less capacity when compared to the causation component, meaning that, at a given value of EDP, the dependent component will likely be already damaged, hence, the dependency on the DS of another component will not be very evident. The greater the overlap, the higher the probability, hence the expected loss, will be, as similarly outlined in Ramirez and Miranda (2009). The example illustrated here may be modified to further pronounce the influence of the correlation on the SLFs by modifying the fragility parameters, but this was deemed a supplementary exercise that is not critical for the scope of the work presented.

Comparison between FEMA P-58 component-based and SLF-based loss assessment

Initially, SLFs were derived based on the component data provided in Tables 1 and 2. No correlation among component DSs was considered. For the PSD-sensitive components, the complete set of three SLFs were derived, corresponding to each of the three stories of the building. For PFA-sensitive components, loss functions for four floors were derived, based on whether the component was sensitive to the PFA of the above floor or the floor upon which it is placed. In addition, PSD-sensitive components were subdivided into separate SLFs based on their orientation (Figure 12). The PACT software (FEMA P-58-3, 2012b) was utilized to conduct the component-based loss estimation, where a total of 200 realizations were used per intensity level and the non-directional conversion factor was assumed to be 1.2.

Apart from record-to-record (RTR) variability and in contrast to the original assessment by O'Reilly et al. (2018), no epistemic uncertainty related to the numerical modeling parameters was considered for simplicity. Consequently, the component-based loss assessment described herein yielded slightly lower loss values with respect to the original study. Several methods are noted when accounting also for modeling uncertainty. One way is to generate demand results from one single deterministic model (the best representation of the building) using many records and increase the variability to include the effect of
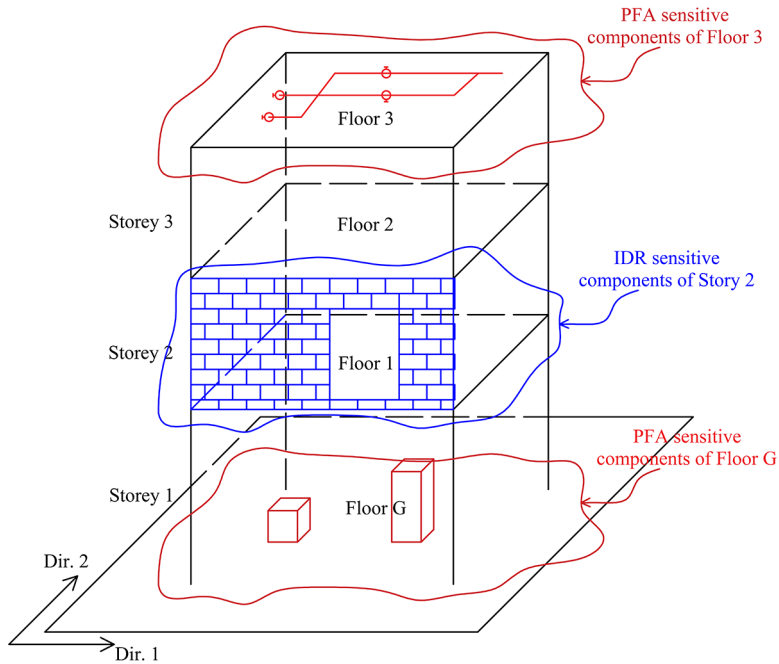
Figure 12. Component group and story loss function identification.

modeling uncertainty. Correlations, medians, and dispersions among the distributions of EDPs at each floor are found and resampled, with the same median but an increased dispersion, accounting for modeling uncertainty. For the specific case study RC frame building, empirical values of modeling uncertainty may be adopted from O'Reilly and Sullivan (2018), for example. Alternatively, different numerical model realizations can be carried out (e.g. different reinforcement values, concrete strength, backbone parameters, etc.), after which nonlinear response-history analyses (NRHA) demands of all models under many records are used to directly account for the modeling uncertainty.

Finally, performance grouping was applied and Equation 5 was used to carry out regression to obtain the SLFs. Probabilistic seismic hazard analysis (PSHA) was performed in O'Reilly et al. (2018) and hazard-consistent ground motion record sets were selected for the site location (the city of Ancona). Figure 13 illustrates the hazard curve for the selected case study building location. The intensity measure (IM) selected was the spectral acceleration, $Sa(T^*)$, at a conditioning period, T^*. Since, the building possesses principal modes of vibration in two orthogonal directions, following a suggestion of FEMA P-58-1 (2012a), a T^* of 0.5 s equaling the arithmetic mean of the two orthogonal modal periods was selected. NRHA were conducted and the results were used to conduct loss assessment using the PACT software for a component-based approach and using the SLFs generated via the proposed toolbox.

Loss assessment approach

The approach proposed by Ramirez and Miranda (2012) was used herein to perform SLF-based loss assessment. The approach takes residual deformations into account to compute
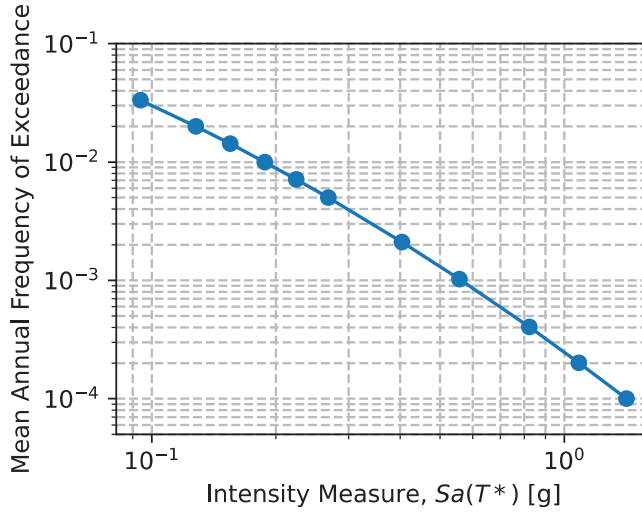
Figure 13. Hazard curve for the site considered in Ancona, Italy.

the probability of the building to be demolished after a seismic event. The economic loss condition on the ground motion intensity is computed as the summation of the following terms: losses due to the building collapse; repair costs due to the building's components being damaged; and losses resulting from the demolition of the building, if it has experienced excessive residual drifts.

The expected total economic loss is the sum of three mutually exclusive, collectively exhaustive events, conditioned on a ground motion IM, and is given by Equation 8:

$$
\begin{aligned}
E[L_T|\mathrm{IM}] = {} & E[L_T|\mathrm{NC} \cap R, IM]P(NC \cap R|IM) \\
& + E[L_T|\mathrm{NC} \cap D]P(NC \cap D|IM) + E[L_T|C]P(C|IM)
\end{aligned}
\tag{8}
$$

where $E[L_T|NC \cap R, IM]$ is the expected total loss in the building given no collapse and the components are repaired given the ground motion IM, which is the quantity output from the SLFs; $E[L_T|NC \cap D]$ is the expected loss given no collapse but the building is demolished, and $E[L_T|C]$ is the expected loss when the building has collapsed. The weights in Equation 8 are described as follows: $P(NC \cap R, IM)$ is the probability of the building not collapsing but being repaired given the ground motion IM; $P(NC \cap D|IM)$ is the probability of the building not collapsing but being demolished due to excessive residual drifts given the ground motion IM, and $P(C|IM)$ is the probability of the building collapsing given the ground motion IM. Equation 8 can be rewritten as Equation 9:

$$
\begin{aligned}
E[L_T|IM] = {} & E[L_T|\mathrm{NC} \cap R, IM]P(R|NC, IM)P(NC|IM) \\
& + E[L_T|\mathrm{NC} \cap D]P(D|NC, IM)P(NC|IM) + E[L_T|C]P(C|IM)
\end{aligned}
\tag{9}
$$

where $P(R|NC, IM)$ and $P(NC|IM)$ are the probabilities that the building will be repaired given no collapse, and that the building did not collapse, respectively, given the ground motion IM; $P(D|NC, IM)$ is the probability of the building to be demolished, given the ground motion IM. The probability of demolishing the building given no collapse at a
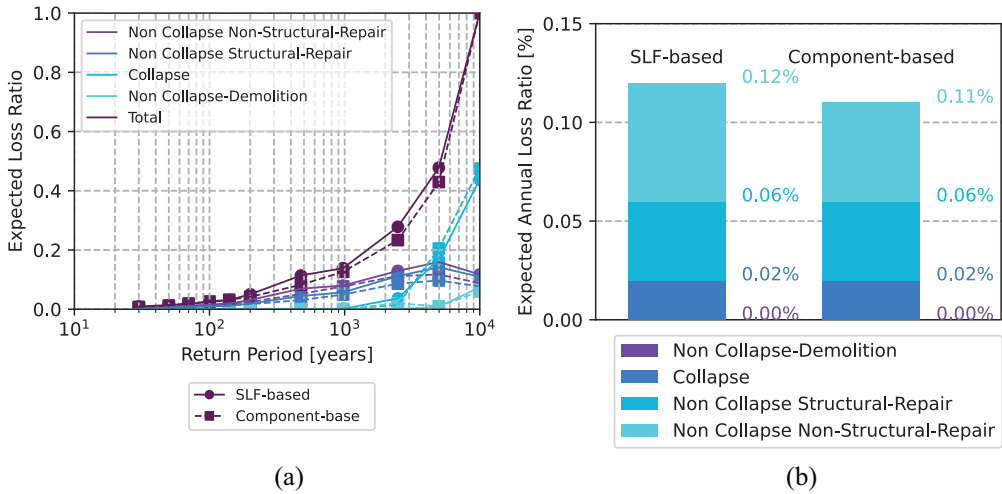
Figure 14. (a) Vulnerability curves and (b) expected annual loss ratio showing the breakdown between different contributors in a comparative assessment between an SLF-based and component-based approach.

ground motion IM is computed as a function of residual PSD (RPSD) following the recommendations of FEMA P-58-1 (2012a). For the case study building, $P(D|RPSD)$ was assumed to be lognormally distributed with a median of 0.015 and a logarithmic standard deviation of 0.3 (Ramirez and Miranda, 2012).

Assessment results

Loss assessment was carried out based on the SLFs developed using the proposed toolbox. Similar to the component-based approach utilized by O'Reilly et al. (2018), a 60% threshold was set during the loss assessment, beyond which the total replacement cost of ã 3,929,937 was assumed for the building. The EAL was computed for the case study building by integrating the vulnerability curve, expressed in terms of expected direct economic loss as a function of IM, with the site hazard curve defined according to Equation 10:

$$EAL = \int E[L_T|\text{IM}] \left| \frac{d\lambda}{dIM} \right| dIM \tag{10}$$

where $d\lambda/dIM$ is the mean annual frequency of the ground motion IM. Given the already identified expected total loss via Equation 9, the EAL disaggregated by cost type, along with the vulnerability curve, is presented in Figure 14. The EAL computed utilizing SLFs was 0.12%, which is slightly higher when compared to the one computed via the FEMA P-58 component-based approach, which was 0.11%. As observed in Figure 14a, the main contribution to the EAL difference comes from the non-structural performance group. Even though the vulnerability curves are quite similar (Figure 14a), at lower intensity levels, differences can be observed, which are predominantly due to the difficulty in ensuring exact fitting of the regression function (Equation 5) in capturing the costs associated with low IM levels regarding non-structural repair cost contributions, resulting in an inevitable EAL difference between the two approaches.
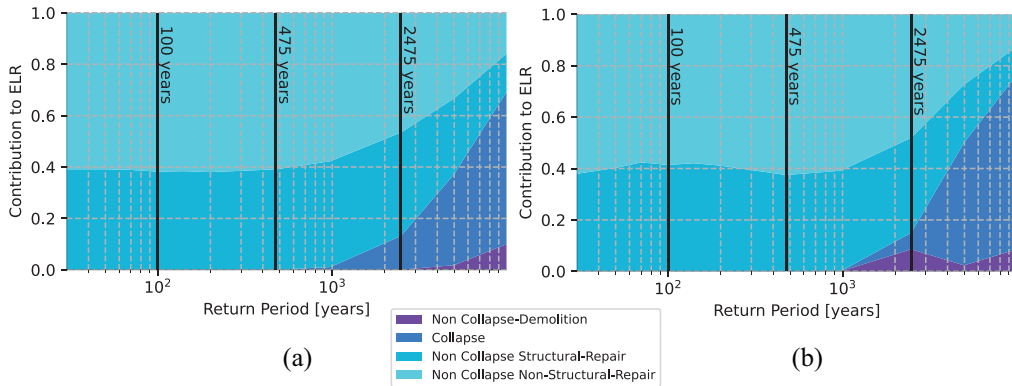
Figure 15. Relative contribution to expected loss with respect to increasing return period for an (a) SLF-based approach and (b) component-based approach. As reference points, the 100-, 475-, and 2475-year return periods have been annotated on each plot.

Finally, Figure 15 provides the relative contributions to the vulnerability curves as a function of the return period. As observed, the main contributors at low hazard levels (i.e. low return period) are the non-structural and structural repair costs. This reinforces the observation that structural repair cost contributions are lower in the component-based approach in comparison to the SLF-based approach. With increasing return period, the repair cost due to damage to structural components reduces, while the repair cost due to damage to non-structural components remains relatively stable. On the contrary, the contribution from collapse and demolition to the expected loss ratio (ELR) starts increasing, however, remains relatively low, compared to repair costs. While it is not possible to compare these losses to real observations for the considered case study building, Del Vecchio et al. (2020) presented actual repair costs of RC residential buildings damaged by the 2009 earthquake in L'Aquila, Italy that can provide some useful comparison. In that study, around 90% of the total replacement cost was attributed to the non-structural components, while structural components averaged around 3%–10%. These differ from the respective contributions derived from both component-based and SLF-based assessment methods employed, which are around 38% and 62% at low return periods for structural and non-structural components, respectively. The main reason for this difference could be attributed to exterior masonry infill panels, which contribute notably to the losses, and were classified as structural components within this study while considered a non-structural element by Del Vecchio et al. (2020) This is not deemed a major concern, as it depends on the practitioner's choice for those functions when carrying out loss assessment. The focus of the present study, though, is the comparison of loss outputs between SLF-based and component-based loss assessment frameworks, which indicates how the SLFs produced using the proposed toolbox are capable of providing component-based-quality predictions of loss that would be obtained with more conventional software such as PACT.

Summary and conclusion

Given the lack of available tools to develop SLFs to fit any user's own specific needs, this article aimed to fill the gap by introducing an SLF generation toolbox for seismic design and assessment of buildings. This was described with step-by-step implementation and was validated through its application to a case study school building in a comparative

study with the more rigorous component-based loss assessment described in FEMA P-58. In addition, the toolbox was applied to a single story, with the goal to compare the effects of assumptions where component DSs were considered independent and where the dependency of DSs of different components was assumed. The main observations from this study are as follows:

- The toolbox is capable of accounting for component correlation and can avoid the problem of double counting of repair costs that is sometimes encountered in practice. The toolbox was applied to a single story to investigate how the consideration of component dependency and interaction impacts in the observed vulnerability when compared to the independency assumption.
- SLFs were developed for the entire case study school building accounting for the response in both directions and a subsequent loss assessment was carried out. Results were compared to a component-based loss assessment approach with a good match in EAL between the two approaches.
- This close matching of the SLF-based loss estimates to the detailed FEMA P-58 component-based loss was also observed in the distribution of the losses among performance groups per intensity. This comparison highlights the validity of the developed tool and its accurate applicability for the intended scopes initially outlined
- In addition to typical objective of performing loss assessment on existing buildings, SLFs could act as an important tool for new designs within novel risk-based design approaches. Simplified relationships between expected losses and structural demands (i.e. SLFs) could be integrated and used to when designing new structures to limit the potential for excessive monetary losses due to building damage, as described in O'Reilly and Calvi (2019), for example.

While the developments outlined in this work have shown an ease of SLF development via the proposed toolbox and illustrated its accuracy with respect to more robust approaches to loss estimation, some future extension may be made. These include the consideration of interactions between components physically located at different stories of a building or associated with different performance groups. A tool for quick manipulation and browsing of component data may also be foreseen to allow the user to add or remove components and visualize all existing components. In addition, the toolbox currently operates on only two types of distributions (i.e. normal and lognormal). Future extensions could foresee the possibility of including other, such as truncated distributions or multi-modal distributions, that would add flexibility to the toolbox. These possible additional features would be possible to implement, considering the object-oriented programming used to develop the SLF generation toolbox structured through modular class definitions in Python.

Declaration of conflicting interests

Funding

ORCID iDs

Davit Shahnazaryan https://orcid.org/0000-0002-0529-5763
Gerard J O'Reilly https://orcid.org/0000-0001-5497-030X

References

American Society of Civil Engineers (ASCE) 7-16 (2016) *Minimum Design Loads for Buildings and Other Structures*. Reston, VA: ASCE.

Aschheim M and Black EF (2000) Yield point spectra for seismic design and rehabilitation. *Earthquake Spectra* 16(2): 317–335.

Aslani H and Miranda E (2005) Fragility assessment of slab-column connections in existing non-ductile reinforced concrete buildings. *Journal of Earthquake Engineering* 9(6): 777–804.

Balboni B (2007) *2007 RSMeans Square Foot Costs*. Kingston, MA: RSMeans.

Cardone D (2016) Fragility curves and loss functions for RC structural components with smooth rebars. *Earthquakes and Structures* 10(5): 1181–1212.

Cardone D and Perrone G (2015) Developing fragility curves and loss functions for masonry infill walls. *Earthquakes and Structures* 9(1): 257–279.

Chiozzi A and Miranda E (2017) Fragility functions for masonry infill walls with in-plane loading. *Earthquake Engineering & Structural Dynamics* 46(15): 2831–2850.

Comité Européen de Normalisation (CEN) EN 1998-1 (2004) *Eurocode 8: Design of Structures for Earthquake Resistance—Part 1: General Rules, Seismic Actions and Rules for Buildings*. Brussels: CEN.

Cornell CA (1996) Calculating building seismic performance reliability: A basis for multi-level design norms. In: *Proceedings of the 11th world conference on earthquake engineering*, Acapulco, Mexico, 23–28 June, p. 8. Oxford: Pergamon Press.

Cornell CA and Krawinkler H (2003) *Progress and Challenges in Seismic Performance Assessment*. Berkeley, CA: Pacific Earthquake Engineering Research Center (PEER), University of California, Berkeley.

Del Gaudio C, De Risi MT, Ricci P and Verderame GM (2019) Empirical drift-fragility functions and loss estimation for infills in reinforced concrete frames under seismic loading. *Bulletin of Earthquake Engineering* 17(3): 1285–1330.

Del Vecchio C, Di Ludovico M and Prota A (2020) Repair costs of reinforced concrete building components: From actual data analysis to calibrated consequence functions. *Earthquake Spectra* 36(1): 353–377.

Federal Emergency Management Agency (FEMA) P-58-1 (2012a) *Seismic Performance Assessment of Buildings: Volume 1—Methodology*. Washington, DC: FEMA.

Federal Emergency Management Agency (FEMA) P-58-3 (2012b) *Seismic Performance Assessment of Buildings: Volume 3—Performance Assessment Calculation Tool (PACT)*. Washington, DC: FEMA.

Kennedy RC and Short SA (1994) *Basis for Seismic Provisions of DOE-STD-1020*. Livermore, CA: Lawrence Livermore National Laboratory.

Krawinkler H, Zareian F, Medina RA and Ibarra LF (2006) Decision support for conceptual performance-based design. *Earthquake Engineering & Structural Dynamics* 35(1): 115–133.

Luco N, Ellingwood BR, Hamburger RO, Hooper JD, Kimball JK and Kircher CA (2007) Risk-targeted versus current seismic design maps for the conterminous United States. In: *Structural Engineers Association of California (SEAOC) 2007 convention proceedings*, Squaw Creek, CA, 26–29 September, pp. 1–13. Sacramento, CA: SEAOC.

NZS 1170.5:2004 (2004) *Structural Design Actions—Part 5: Earthquake Actions*. Wellington: Standards New Zealand.

O'Reilly GJ and Calvi GM (2019) Conceptual seismic design in performance-based earthquake engineering. *Earthquake Engineering & Structural Dynamics* 48(4): 389–411.

O'Reilly GJ and Sullivan TJ (2018) Quantification of modelling uncertainty in existing Italian RC frames. *Earthquake Engineering & Structural Dynamics* 47(4): 1054–1074.

O'Reilly GJ, Perrone D, Fox M, Monteiro R and Filiatrault A (2018) Seismic assessment and loss estimation of existing school buildings in Italy. *Engineering Structures* 168: 142–162.

O'Reilly GJ, Perrone D, Fox M, Monteiro R, Filiatrault A, Lanese I and Pavese A (2019) System identification and seismic assessment modeling implications for Italian school buildings. *Journal of Performance of Constructed Facilities* 33(1): 04018089.

O'Reilly GJ, Sullivan TJ and Filiatrault A (2017) Implications of a more refined damage estimation approach in the assessment of RC frames. In: *Proceedings of the 16th world conference on earthquake engineering*, Santiago, 9–13 January.

Ottonelli D, Cattari S and Lagomarsino S (2020) Displacement-based simplified seismic loss assessment of masonry buildings. *Journal of Earthquake Engineering* 24: 23–59.

Papadopoulos AN, Vamvatsikos D and Kazantzi AK (2019) Development and application of FEMA P-58 compatible story loss functions. *Earthquake Spectra* 35(1): 95–112.

Perrone G, Cardone D, O'Reilly GJ and Sullivan TJ (2019) Developing a direct approach for estimating expected annual losses of Italian buildings. *Journal of Earthquake Engineering*. Epub ahead of print 19 September. DOI: 10.1080/13632469.2019.1657988.

Ramirez CM and Miranda E (2009) Building-specific loss estimation methods & tools for simplified performance-based earthquake engineering. *Blume Center report, Blume Center, Stanford University, Stanford, CA*, May.

Ramirez CM and Miranda E (2012) Significance of residual drifts in building earthquake loss estimation. *Earthquake Engineering & Structural Dynamics* 41: 1477–1493.

Ruiz-García J and Negrete M (2009) Drift-based fragility assessment of confined masonry walls in seismic zones. *Engineering Structures* 31(1): 170–181.

Sassun K, Sullivan TJ, Morandi P and Cardone D (2016) Characterising the in-plane seismic performance of infill masonry. *Bulletin of the New Zealand Society for Earthquake Engineering* 49(1): 98–115.

Shahnazaryan D, O'Reilly GJ and Monteiro R (2021) Storey loss function generator. DOI: 10.5281/zenodo.4897798.

Shahnazaryan D and O'Reilly GJ (2021) Integrating expected loss and collapse risk in performance-based seismic design of structures. *Bulletin of Earthquake Engineering* 19(2): 987–1025.

Silva A, Castro JM and Monteiro R (2020a) A rational approach to the conversion of FEMA P-58 seismic repair costs to Europe. *Earthquake Spectra* 36(3): 1607–1618.

Silva A, Macedo L, Monteiro R and Castro JM (2020b) Earthquake-induced loss assessment of steel buildings designed to Eurocode 8. *Engineering Structures* 208: 110244.

Sullivan TJ (2016) Use of limit state loss versus intensity models for simplified estimation of expected annual loss. *Journal of Earthquake Engineering* 20(6): 954–974.

Vamvatsikos D and Aschheim MA (2016) Performance-based seismic design via yield frequency spectra‡. *Earthquake Engineering & Structural Dynamics* 45(11): 1759–1778.

Žižmond J and Dolšek M (2019) Formulation of risk-targeted seismic action for the force-based seismic design of structures. *Earthquake Engineering & Structural Dynamics* 48: 1406–1428.